DEEP LEARNING FOR EMBEDDED IMAGE COMPRESSION IN EARTH OBSERVATION

Vinicius ALVES DE OLIVEIRA
PhD defense, IRIT/ENSEEIHT, Toulouse

Supervisor	Marie CHABERT	Professor at IRIT/INP-ENSEEIHT, Toulouse
Co-supervisor	Charly POULLIAT	Professor at IRIT/INP-ENSEEIHT, Toulouse
Co-supervisor	Thomas OBERLIN	Professor at ISAE-SUPAERO, Toulouse

University of Toulouse, IRIT/INP-ENSEEIHT

October 21th, 2022

Satellite imaging system

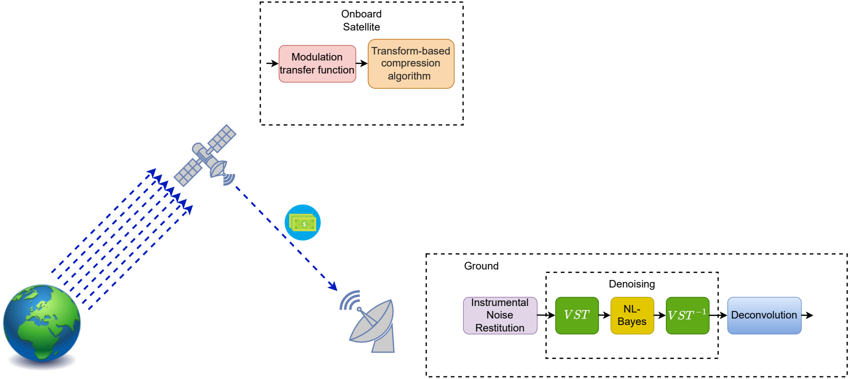

Figure: Basic stages of the Pléiades image processing pipeline[1].

1- [Del+19] J.-M. Delvit and others, *"A pipeline to improve compressed image quality"*. In: ICSO (2018).

Satellite imaging system: onboard compression

Context:

- Increasing spectral and spatial resolution of satellite images.
- Limited communications capabilities.
- Computational limitations onboard the satellite.

Wavelet-based compression methods:

- Consultative committee for space data systems standard (CCSDS) 122.0-B-2: compromise between complexity and performance[2].
- CNES-proprietary compressor with fixed quality per block[3].

2- [Boo17] B. Book, *"Image Data Compression CCSDS 122.0-B-2"*, In: CCSDS Secretariat (2017).

3- [Thi+16] C. Thiebaut and others, *"Performances of a CCSDS-based algorithm for quality- controlled compression on Earth observation missions"*. In: OBPDC (2016).

Image compression using wavelet transform

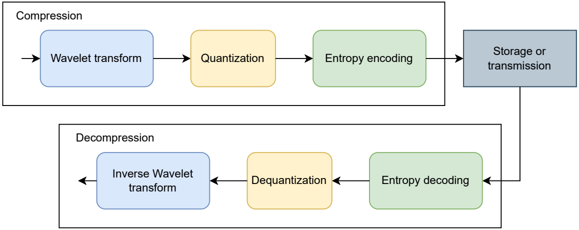

Figure: Block diagram of lossy image compression using wavelet transform.

- Good transform:
  - Decorrelates well[4].
  - Efficient encoding results from the precise estimation of the probability distribution (PDF) of the quantized coefficients.
- Limitations:
  - Optimal only under strong assumptions about the underlying distribution of image data.
  - Visual artifacts such as ringing and blur.

4- [TMB05] D. Tretter and others, *"Multispectral image coding"*, In: The Image and Video Processing Handbook (2005).

Problematic of the thesis

Motivation:

- Machine learning (ML) vs. model-based techniques.
- Neural networks (NNs) as powerful data-driven tools.
- Non-linear transform.

Methods towards data-driven compression:

- Convolutional neural networks (CNNs)[5].
- Convolutional Autoencoders.

Problems :

- High computational complexity.
- Particularities of lossy image compression.

5- [Ben09] Y. Bengio, *"Learning deep architectures for AI"*, In: Foundations and trends in Machine Learning (2009).

Convolutional neural networks (CNNs)

Principle:

- Commonly applied to analyze images[6].
- Convolution operation.
- Shift-invariant, based on the shared-weight architecture.
- Widely impacted image processing.

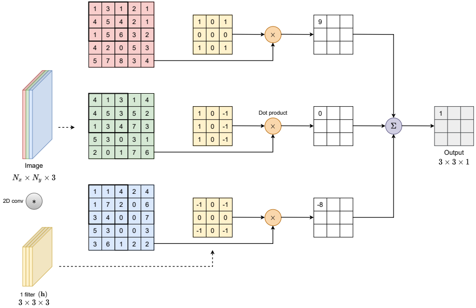

Figure: Illustration of the convolutional operation.

6- [Ben09] Y. Bengio, *"Learning deep architectures for AI"*, In: Foundations and trends in Machine Learning (2009).

Convolutional autoencoders

Principle:

- Learn descriptive representation in lower dimension[7].
- Non-linear transform.
- Output reconstructed images.

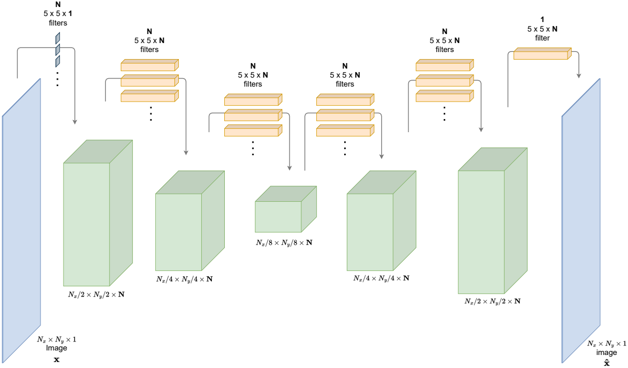

Figure: Illustration of a convolutional autoencoder.

7- [Ben09] Y. Bengio, *"Learning deep architectures for AI"*, In: Foundations and trends in Machine Learning (2009).

Outline

1. Learned reduced-complexity onboard satellite image compression
2. Satellite image compression and denoising
3. Conclusion and Perspectives

Outline

1. Learned reduced-complexity onboard satellite image compression[8]
    1.1 End-to-end learned image compression
    1.2 Statistical analysis of the learned transform
    1.3 Propositions
    1.4 Experimental results

8- [Alv+21] V. Alves de Oliveira and others, *"Reduced-Complexity End-to-End Variational Autoencoder for on Board Satellite Image Compression"*, In: Special Issue Remote Sensing Data Compression 13.3 (2021).

End-to-end learned image compression

- Principle: jointly learn a non-linear transform and its underlying statistical distribution to optimize a rate-distortion trade-off.

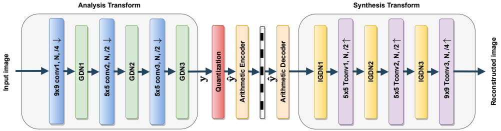

Figure: Architecture of the autoencoder[9].

- Analysis and synthesis transforms:
  - Convolutional layers (downsampling: stride convolutions / upsampling: transposed convolutions).
  - Activation functions: generalized divisive normalization (GDN) (resp. inverse generalized divisive normalization (IGDN)).

where:

- GDN and IGDN: functions implementing an adaptive normalization.

$$GDN(v_i(k,l)) = \frac{v_i(k,l)}{(\beta_i + \sum_{j=1}^{N} \gamma_{ij} v_j^2(k,l))^{1/2}} \text{ for } i = 1, \dots, N,$$

$v_i(k,l)$: spatial location indexed by (k,l) of the output of the i^{th} filter. N: number of channels.

9- [BLS17] J. Ballé and others, *"End-to-end optimized image compression"*. In: ICLR (2017).

End-to-end learned image compression

- Quantized representation:

$$\hat{\mathbf{y}} = Q\left(G_a(\mathbf{x})\right).$$

  G_a: analysis transform.
  Q: uniform scalar quantization with quantization step size equals to 1.

- Reconstructed image:

$$\hat{\mathbf{x}} = G_s(\hat{\mathbf{y}}).$$

  G_s: synthesis transform.

- $p_{\hat{\mathbf{y}}}(\hat{\mathbf{y}})$: discrete probability distribution of the quantized representation.
- Lossless entropy coder encodes $\hat{\mathbf{y}}$ knowing $p_{\hat{\mathbf{y}}}(\hat{\mathbf{y}})$.

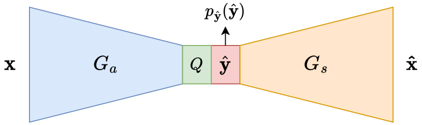

Figure: End-to-end autoencoder for learned image compression.

Problem formulation

Rate-distortion optimization:

$$\hat{\theta}_{G_a}, \hat{\theta}_{G_s}, \hat{\theta}_{p_{\hat{y}}} = \underset{\theta_{G_a}, \theta_{G_s}, \theta_{p_y}}{\arg\min} \; \lambda D(\mathbf{x}, \hat{\mathbf{x}}) + R(\hat{\mathbf{y}}),$$

- $\theta_{G_a}, \theta_{G_s}, \theta_{p_{\hat{y}}}$: set of parameters for the analysis transform, synthesis transform and entropy model, respectively.

Motivation: rate-distortion trade-off.

$D(\mathbf{x}, \hat{\mathbf{x}})$: distortion between the original image and the reconstructed image.

$R(\hat{\mathbf{y}})$: number of bits/pixel used to encode $\hat{\mathbf{y}}$.

λ: controls the trade-off.

Problem formulation

- Smallest bit-rate is given by the Shannon cross entropy:

$$R(\hat{\mathbf{y}}) = H(\hat{\mathbf{y}}) = \mathbb{E}_{\hat{\mathbf{y}} \sim m} \left[-log_2 p_{\hat{\mathbf{y}}}(\hat{\mathbf{y}}) \right].$$

$m(\hat{\mathbf{y}})$: actual discrete probability distribution of $\hat{\mathbf{y}}$

- Rate increases with the mismatch between $p_{\hat{\mathbf{y}}}(\hat{\mathbf{y}})$ and $m(\hat{\mathbf{y}})$.

Relaxation to allow optimization (during training):

- Quantization approximated using additive uniform noise[10]:

$$\tilde{y} = y + \eta \quad , \quad \eta \sim \mathcal{U}\left(-0.5, +0.5\right).$$

$$p_{\tilde{y}}(\tilde{y}) = p_y(y) * p_\eta$$

η: quantization noise.
p_η: distribution of the quantization noise.
$p_{\tilde{y}}(\tilde{y})$: continuous approximation of $p_{\hat{y}}(\hat{y})$.

10- [BLS17] J. Ballé and others, *"End-to-end optimized image compression"*. In: ICLR (2017).

Two reference learning-based architectures

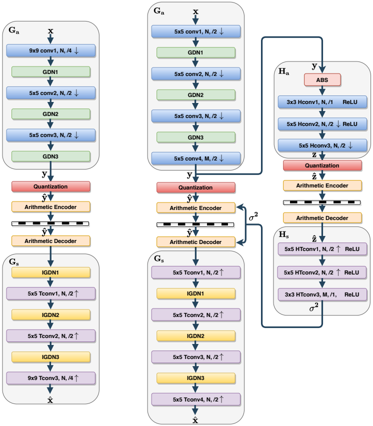

Figure: Architecture of the autoencoder[11] (AE−1) (**left**) and of the variational autoencoder[12] (AE−2) (**right**).

11- [BLS17] J. Ballé and others, *"End-to-end optimized image compression"*. In: ICLR (2017).

12- [Bal+18] J. Ballé and others, *"Variational image compression with a scale hyperprior"*. In: ICLR (2018).

Rate estimation for AE−1

Entropy model:

- Fully factorized model[13]:

$$p_{\tilde{\mathbf{y}}|\boldsymbol{\psi}}(\tilde{\mathbf{y}}|\boldsymbol{\psi}) = \prod_j \prod_i p_{\tilde{y}_{i_j}|\psi_j}(\tilde{y}_{i_j}).$$

  i runs over all spatial locations within a channel j.
  $\boldsymbol{\psi}_j$: distribution model parameter vector associated with each channel - fixed after training.

- Hypothesis:
  - $\tilde{\mathbf{y}}$ assumed independent and identically distributed within each channel.
  - Channels are assumed independent of each other.

- Non-parametric statistical model.

- Drawback: not adaptive to different images.

13- [BLS17] J. Ballé and others, *"End-to-end optimized image compression"*. In: ICLR (2017).

Rate estimation for AE−2

Entropy model:

- Hyperprior model[14]:

$$\tilde{y}_{ij}|\tilde{\mathbf{z}} \sim \mathcal{N}\left(0, {\sigma_{ij}}^2\right) * \mathcal{U}\left(-0.5, +0.5\right).$$

- Observation: spatial dependency in $\tilde{\mathbf{y}}$.
- Auxiliary autoencoder.
- $\tilde{\mathbf{z}}$: auxiliary random variables.
- $\tilde{y}_{ij}$ conditioned to $\tilde{\mathbf{z}}$ is independent.
- Advantages:
  - Better modeling.
  - Adaptive to different images.
- Drawbacks:
  - Increase in complexity.
  - Transmission of $\tilde{\mathbf{z}}$ as side information.

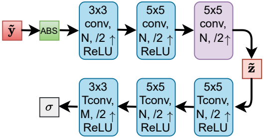

14- [Bal+18] J. Ballé and others, *"Variational image compression with a scale hyperprior"*. In: ICLR (2018).

Outline

Dataset of simulated images

- 12-bit simulated Pléiades panchromatic images (originally of size 586×586) provided by the CNES.
  - Various landscapes (i.e. desert, water, forest, industrial, cloud, port, rural, urban).
- Well-known image acquisition parameters[15].
- Obtained from an airborne in a 10cm resolution, but downsampled to 70cm.
- Training dataset $(116$ images$)$ $|$ test dataset $(16$ images$)$.

Figure: Simulated 12-bit Pléiades images.

15- [Del+19] J.-M. Delvit and others, *"A pipeline to improve compressed image quality"*. In: ICSO (2018).

Statistical analysis of the learned transform

- Prior knowledge to simplify the entropy model?
- Main autoencoder[16] ($N = 128$ and $M = 192$) - fully factorized model[17].
- Kolmogorov-Smirnov goodness-of-fit test[18].
- Most features follow a Laplacian distribution defined by:

$$f(\zeta, \mu, b) = \frac{1}{2\lambda} exp\left(-\frac{|\zeta - \mu|}{b}\right) \text{ for } \zeta \in \mathbb{R}.$$

- As an illustration:

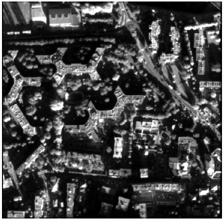

Figure: Simulated 12-bit Pléiades image of Cannes with size 512×512 and resolution $70cm$.

16- [Bal+18] J. Ballé and others, *"Variational image compression with a scale hyperprior"*. In: ICLR (2018).
17- [BLS17] J. Ballé and others, *"End-to-end optimized image compression"*. In: ICLR (2017).
18- [PG81] J. W. Pratt and J. D. Gibbons, *"Kolmogorov-Smirnov two-sample tests"*. In: Concepts of Nonparametric Theory (1981).

Statistical analysis of the learned transform

- $\mathbf{94}\%$ of the features of this image follows a Laplacian distribution with a significance level $\alpha = 5\%$.

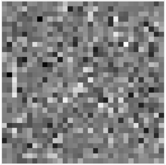

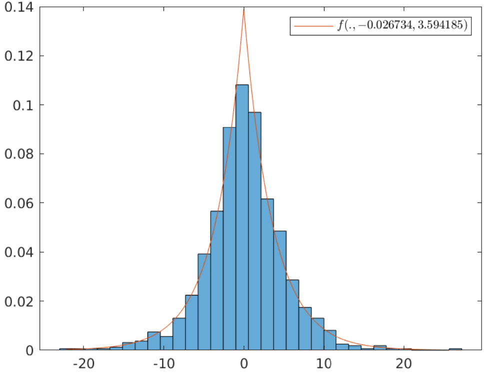

Figure: First feature of Cannes image representation, its normalized histogram with Laplacian fitting.

Statistical analysis of the learned transform

- The remaining non-Laplacian feature maps (6% of the maps for this example) stay close to the Laplacian distribution.

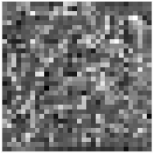

(**a**) 19^{th} feature.

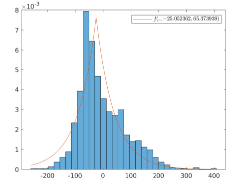

(**b**) Normalized histogram and Laplacian fitting.

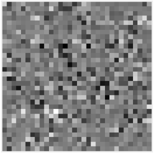

(**c**) 55^{th} feature.

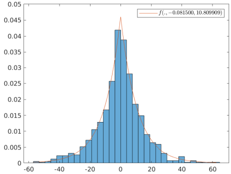

(**d**) Normalized histogram and Laplacian fitting.

Figure: Normalized histogram of the j^{th} feature map and Laplacian fitting $f(., \mu, b)$.

Simplified entropy model

- Objective:
  - Compromise between simplicity and performance.
  - Adaptability to the input image.
- Proposal:
  - Simplified parametric model for all elements y_{i_j} of the j^{th} feature for $i_j \in I_j$, where I_j denotes the set of indexes covering the j^{th} feature:

$$y_{i_j} \sim \text{Laplace}(0,\ b_j)$$

$$\text{with: } b_j = \sqrt{Var(y_{i_j})/2}$$

  - The scale parameter (b_j) is estimated for each feature of each input image.

Simplified entropy model

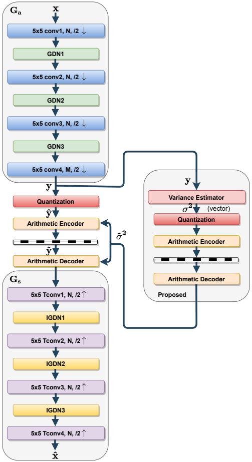

Figure: Proposed architecture after entropy model simplification: main autoencoder[19] (AE−2−L) (**left column**) and simplified entropy model (**right column**)[20].

19- [Bal+18] J. Ballé and others, *"Variational image compression with a scale hyperprior"*. In: ICLR (2018).
20- [Alv+21] V. Alves de Oliveira and others, *"Reduced-Complexity End-to-End Variational Autoencoder for on Board Satellite Image Compression"*, In: Remote Sensing 13.3 (2021).

Reduction of the number of filters

- N: number of filters/channels (apart from the before-bottleneck layer).
- Higher M (bottleneck size) has to be maintained - wide bottleneck strategy[21].
- Proposal:
  - Variational autoencoder: `AE-2-H-C` from $\underline{N = 128/192}$ to $\underline{N = 64}$.
  - Bottleneck size maintained ($M = 192$ or $M = 320$).
- Metrics: number of parameters N_p and floating point operations per pixel (FLOPp).
- Positive impact on the memory occupancy.

21- [Bal+18] J. Ballé and others, *"Variational image compression with a scale hyperprior"*. In: ICLR (2018).

Implementation setup

- Two propositions:
  1. Entropy model simplification.
  2. Reduction of the number of filters composing the convolutional layers.
- Simulation experiments using Tensorflow:
  - Simulated 12-bit Pléiades panchromatic images provided by the CNES.
  - Rate and distortion measurements averaged on the test dataset for a given value of λ.
  - Metrics: MSE and multiscale structural similarity index (MS-SSIM).
- Proposed/reference methods:
  - `AE-2-L-C`[22]: architecture featuring the simplified entropy model.
  - `AE-2-H-C`[23].
  - `AE-1-NP-C`[24].
  - CCSDS 122.0-B[25] / JPEG2000.

22- [Alv+21] V. Alves de Oliveira and others, *"Reduced-Complexity End-to-End Variational Autoencoder for on Board Satellite Image Compression"*, In: Remote Sensing 13.3 (2021).

23- [Bal+18] J. Ballé and others, *"Variational image compression with a scale hyperprior"*. In: ICLR (2018).

24- [BLS17] J. Ballé and others, *"End-to-end optimized image compression"*. In: ICLR (2017).

25- [Boo17] B. Book, *"Image Data Compression CCSDS 122.0-B-2"*, In: CCSDS Secretariat (2017).

Performance analysis

Impact of the number of filter reduction on performance for low bit rates:
Apart from the before-bottleneck layer

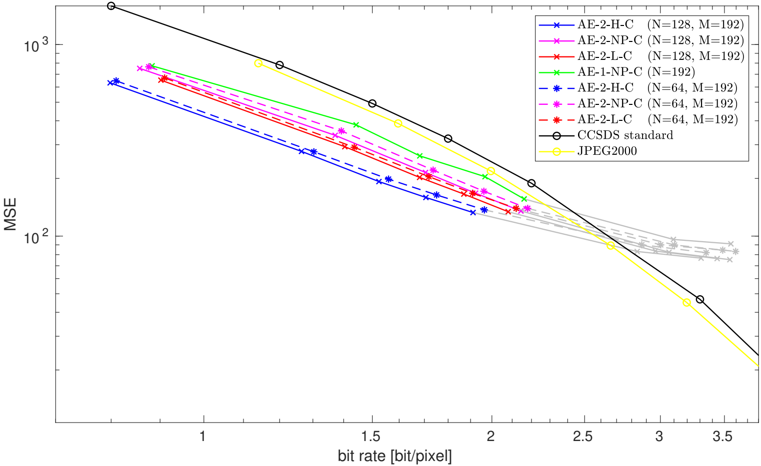

Figure: Rate-distortion curves for the considered methods in terms of MSE (log-log scale).

Performance analysis

Impact of the number of filter reduction on performance for low bit rates:
Apart from the before-bottleneck layer

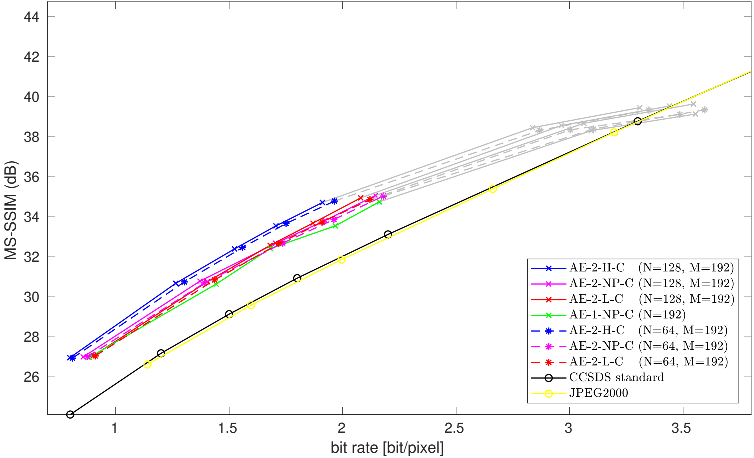

Figure: Rate-distortion curves for the considered methods in terms of MS-SSIM (dB) (derived as $-10\log_{10}(1-\text{MS-SSIM})$).

Performance analysis

Impact of the number of filter reduction on performance for high bit rates:
Apart from the before-bottleneck layer

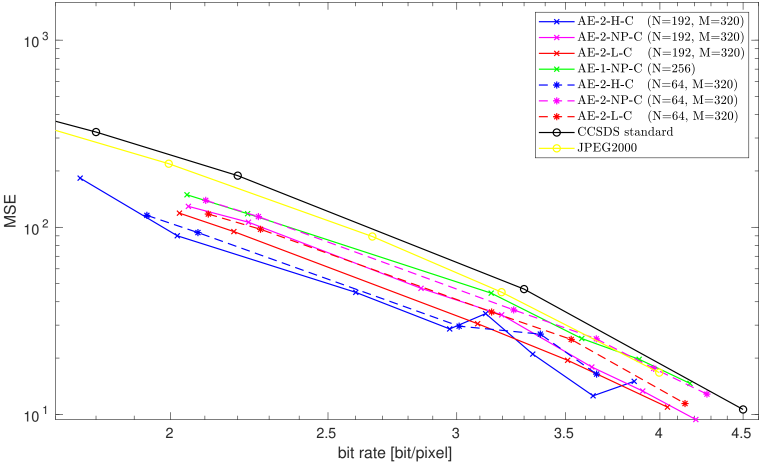

Figure: Rate-distortion curves for the considered methods in terms of MSE (log-log scale).

Performance Analysis

Impact of the number of filter reduction on performance:
The before-bottleneck layer

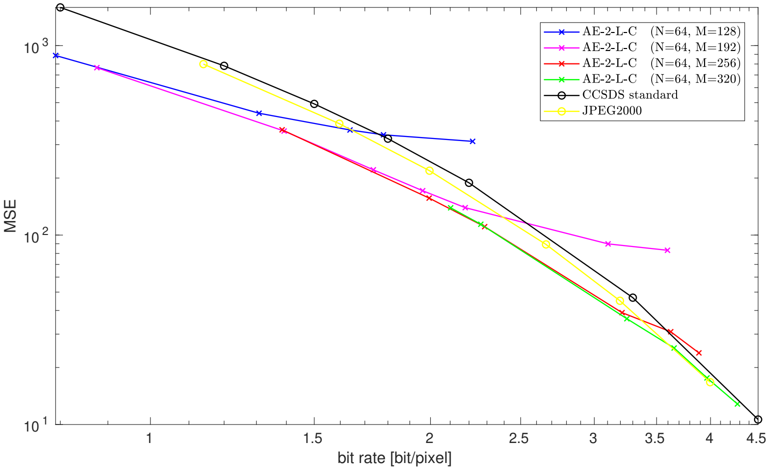

Figure: Impact of the bottleneck size in terms of MSE in (log-log scale).

Performance analysis

Impact of the number of filter reduction on complexity:
Apart from the before-bottleneck layer

Table: Comparative complexity of the global architectures - low rates (up to 2 bits/pixel).

Method	Parameters	FLOPp	Relative
AE-2-H-C (N=128, M=192)	5.0551×10^6	1.9115×10^5	1.00
AE-2-H-C (N=64, M=192)	1.6839×10^6	5.2264×10^4	0.27
AE-2-L-C (N=64, M=192)	1.0527×10^6	5.0774×10^4	0.265

Table: Comparative complexity of the global architectures - high rates (above 2 bits/pixel).

Method	Parameters	FLOPp	Relative
AE-2-H-C (N=192, M=320)	11.7852×10^6	4.3039×10^5	1.00
AE-2-H-C (N=64, M=320)	1.6840×10^6	5.6966×10^4	0.13
AE-2-L-C (N=64, M=320)	1.0527×10^6	5.4774×10^4	0.1273

Performance analysis

Impact of the entropy model simplification on complexity:

Table: Reduction of the encoder complexity induced by the Laplacian entropy model on the coding part - low rates (up to 2 bits/pixel).

Method	Parameters	FLOPp	Relative
`AE-2-H-C (N=64, M=192)`	1.1577×10^6	1.25×10^4	1
`AE-2-L-C (N=64, M=192)`	0.5264×10^6	1.09×10^4	0.87

Table: Reduction of the encoder complexity induced by the Laplacian entropy model on the coding part - high rates (above 2 bits/pixel).

Method	Parameters	FLOPp	Relative
`AE-2-H-C (N=64, M=320)`	1.7150×10^6	1.3979×10^4	1
`AE-2-L-C (N=64, M=320)`	0.7314×10^6	1.1787×10^4	0.8432

Performance analysis

Subjective image quality assessment:

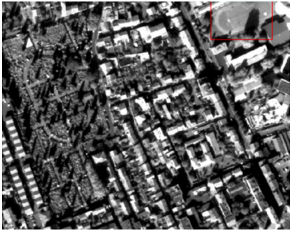

(**a**) Original image.

(**b**) Zoom on the original image.

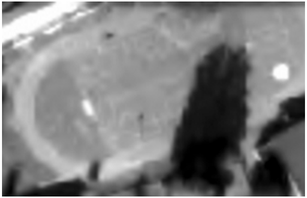

(**c**) Zoom on the CCSDS compressed image.

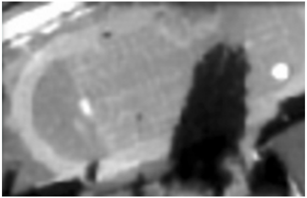

(**d**) Zoom on the end-to-end compressed image.

Figure: Subjective image quality analysis (R = 2.02 bits/pixel).

Outline

26- [Alv+22] V. Alves de Oliveira and others, *"Satellite Image Compression and Denoising With Neural Networks"*, In: IEEE Geoscience and Remote Sensing Letters, vol. 19 (2022).

Combining compression and denoising

- Onboard compression | on ground denoising.

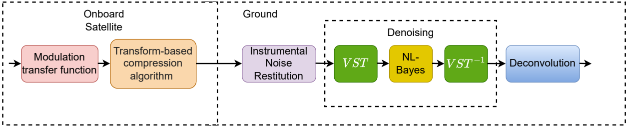

Figure: Pléiades image processing pipeline[27].

- Noise: acquisition + compression.
- Non Local (NL) Bayes denoising:
  - Hypothesis: standard additive noise model.
    - Variance stabilizing transform (VST) + instrumental noise restitution.
  - Patch-based method.
  - Estimate the variability in a group of similar patches to denoise.
  - Computationally expensive.
    - Optimizations proposed by the CNES[28].

27- [Del+19] J.-M. Delvit and others, *"A pipeline to improve compressed image quality"*. In: ICSO (2018).
28- [Mas+18] A. Masse and others, *"Denoising very high resolution optical remote sensing images: Application and optimization of non local bayes method"*. In: IEEE Journal of Selected Topics in Applied Earth Observations and Remote Sensing 11.3 (2018).

Combining compression and denoising

- Data-driven approaches for satellite image compression and denoising.
- Objective:
  - Improve performance.
  - Dispensing from:
    - Manual parameter setting.
    - A priori knowledge of the noise model.
    - Intermediary steps such as variance stabilizing transform (VST) or instrumental noise restitution[29].
- Realistic simulations provide both $\mathbf{I_n}$ and $\mathbf{I_{nf}}$ for the same scene.

  $\mathbf{I_n}$: noisy image.
  $\mathbf{I_{nf}}$: noise-free image.

29- [Del+19] J.-M. Delvit and others, *"A pipeline to improve compressed image quality"*. In: ICSO (2018).

Selected methods from state-of-the-art

End-to-end trainable autoencoder for image compression:

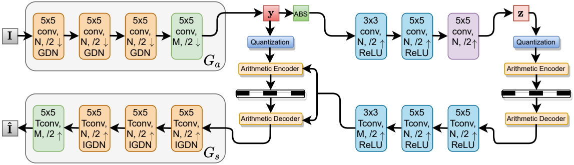

Figure: Architecture of the variational autoencoder[30].

- Relatively shallow architecture.
- Rate-distortion optimization: $\lambda D(\mathbf{x}, \hat{\mathbf{x}}) + R(\hat{\mathbf{y}})$.

30- [Bal+18] J. Ballé and others, *"Variational image compression with a scale hyperprior"*. In: ICLR (2018).

Selected methods from state-of-the-art

Denoising with BRDNet:

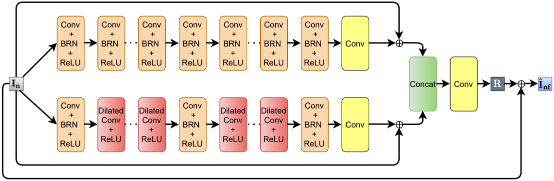

Figure: Architecture of the BRDNet network[31].

- Can adapt to non-standard noise statistical models.
- Deep CNN.
- Batch renormalization (BRN).
- Residual learning (RL) to predict a residual image: $f(\mathbf{I_n}) \backsimeq \mathbf{I_n} - \mathbf{I_{nf}}$.
  $\mathbf{I_n}$: noisy image.
  $\mathbf{I_{nf}}$: noise-free image.
  $f(\mathbf{I_n})$: noise prediction by the DNN.
- Distortion criterion:

$$J(\theta) = D(\mathbf{I_{nf}}, \mathbf{\hat{I}_{nf}}).$$

31- [TXZ20] C. Tian and others, *"Image denoising using deep CNN with batch renormalization"*. In: Neural Networks 121 (2020).

Combining compression and denoising

Proposals:

- Joint compression and denoising (onboard):
  - Compression-dedicated architecture `AE-2-H`.
  - $D(\mathbf{I_{nf}}, G_s(G_a(\mathbf{I_n})))$: distortion between $\hat{\mathbf{I}}_{\mathbf{nf}} = G_s(G_a(\mathbf{I_n}))$ and $\mathbf{I_{nf}}$.

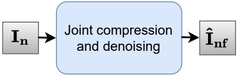

- Sequential compression (onboard) and denoising (on ground):
  - Two architectures: the compression-dedicated one and the denoising-dedicated architecture `BRDNet`.

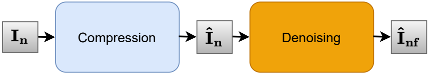

- Denoising as a post-processing (on ground) after joint compression and denoising (onboard):
  - Combines both joint and sequential approaches.

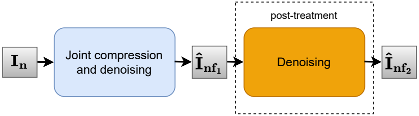

Implementation setup

- Simulation experiments using Tensorflow:
  - Image pairs $\mathbf{I_n}/\mathbf{I_{nf}}$.
  - Metrics: PSNR (dB) and MS-SSIM (dB).
- The reference CNES imaging system[32] - our baseline for compression and denoising performance.
- Proposed/adapted methods:
  - `AE-2-H-CD (N=64, M=320)`: joint compression and denoising.
  - `BRDNet`: BRDNet denoising architecture[33].
- Reference methods:
  - `CNES-C`: CNES compression algorithm[34].
  - `NL-Bayes-CNES`: NL-Bayes denoising algorithm parametrized by the CNES[35].

32- [Del+19] J.-M. Delvit and others, *"A pipeline to improve compressed image quality"*. In: ICSO (2018).
33- [TXZ20] C. Tian and others, *"Image denoising using deep CNN with batch renormalization"*. In: Neural Networks 121 (2020).
34- [Thi+16] C. Thiebaut and others, *"Performances of a CCSDS-based algorithm for quality- controlled compression on Earth observation missions"*. In: OBPDC (2016).
35- [Mas+18] A. Masse and others, *"Denoising very high resolution optical remote sensing images: Application and optimization of non local bayes method"*. In: IEEE Journal of Selected Topics in Applied Earth Observations and Remote Sensing 11.3 (2018).

Performance analysis

Compression and denoising performance:

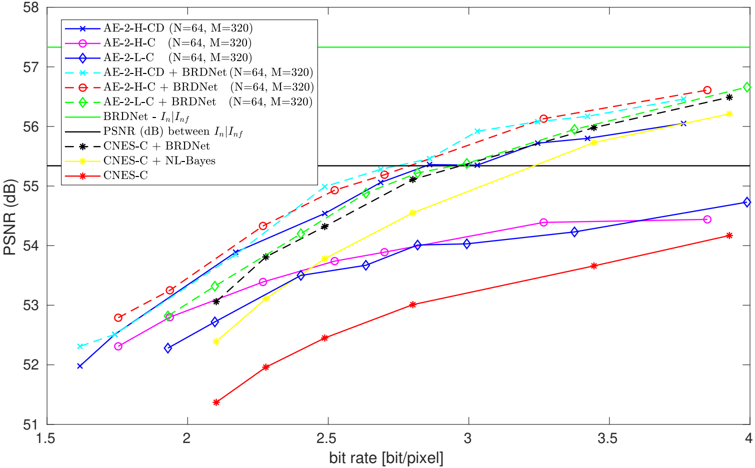

Figure: PSNR (dB) between the output image and the noise-free image ($\mathbf{I_{nf}}$).

Performance analysis

Compression and denoising performance:

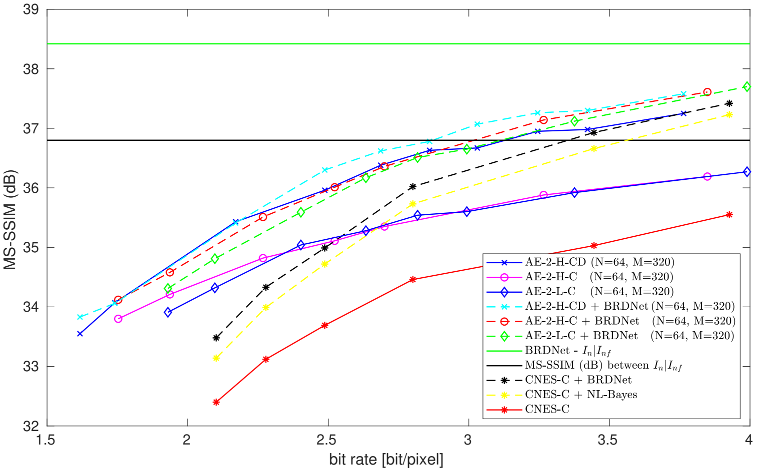

Figure: MS-SSIM (dB) between the output image and the noise-free image ($\mathbf{I_{nf}}$).

Performance analysis

Compression and denoising performance:

Table: Comparative complexity of the considered architectures

Method	Parameters	FLOPp
AE-2-L-C (N=64, M=320)	1052737	5.4774×10^4
BRDNet[36]	1186816	1.1868×10^6

- BRDNet, benefiting from the GPU, is 30 times faster than the NL-Bayes-CNES.

Subjective image quality analysis:

Figure: Result on a test image. (a) CNES-C+NL-Bayes[37]. (b) AE-2-H-C+BRDNet. (c) AE-2-H-CD. (d) Noise-free image ($\mathbf{I_{nf}}$).

36- [TXZ20] C. Tian and others, *"Image denoising using deep CNN with batch renormalization"*. In: Neural Networks 121 (2020).
37- [Del+19] J.-M. Delvit and others, *"A pipeline to improve compressed image quality"*. In: ICSO (2018).

Outline

Conclusion

Learned reduced-complexity satellite image compression:

- Different approaches to adapt the reference learned image compression frameworks[38][39] to onboard satellite image compression:
  - Reduction of the number of filters.
  - Simplified entropy model.
- Outperform the CCSDS standard.

Satellite image compression and denoising with neural networks:

- Data-driven advantages:
  - In terms of performance.
  - Allow to suppress intermediary steps existing in the current CNES imaging system.
- Two approaches:
  - Joint approach performs compression and denoising with a single architecture.
  - Sequential approach compatible with all the architecture simplifications designed for onboard compression.

38- [BLS17] J. Ballé and others, *"End-to-end optimized image compression"*. In: ICLR (2017).

39- [Bal+18] J. Ballé and others, *"Variational image compression with a scale hyperprior"*. In: ICLR (2018).

Perspectives

Feature-dependent entropy model:

- Combine entropy models to handle the diversity of the feature maps.

Desymmetrize the autoencoder to reduce onboard complexity:

- Lighten the analysis transform and eventually compensate by increasing complexity on the synthesis transform.

Hardware implementation:

- Implement and test the new propositions on real satellite hardware.
- Dedicated inference platform/hardware such as Xilinx FPGAs - Vitis™ AI.

Extend the ML-based approaches to other functionalities of a typical satellite imaging system:

- Use the features extracted for image compression in other ML-based functionalities onboard the satellite, such as classification or detection.
- Prospects for extending the ML to the on ground segment.

List of publications

Published journal papers:

[Alv+21]
Alves de Oliveira, V., M. Chabert, T. Oberlin, C. Poulliat, M. Bruno, C. Latry, M. Carlavan, S. Henrot, F. Falzon, and R. Camarero (2021). "Reduced-Complexity End-to-End Variational Autoencoder for on Board Satellite Image Compression," *In Special Issue Remote Sensing Data Compression* 27.jan, 2021, 13(3), 447.
Available on: `https://doi.org/10.3390/rs13030447`

[Alv+22]
Alves de Oliveira, V., M. Chabert, T. Oberlin, C. Poulliat, M. Bruno, C. Latry, M. Carlavan, S. Henrot, F. Falzon, and R. Camarero (2022). "Satellite Image Compression and Denoising With Neural Networks," in IEEE Geoscience and Remote Sensing Letters, vol. 19, pp. 1-5, 2022, Art no. 4504105.
Available on: `https://doi.org/10.1109/LGRS.2022.3145992`

International conferences:

[Alv+20]
Alves de Oliveira, V., T. Oberlin, M. Chabert, C. Poulliat, B. Mickael, C. Latry, M. Carlavan, S. Henrot, F. Falzon, and R. Camarero (2020). "Simplified entropy model for reduced-complexity end-to-end variational autoencoder with application to on-board satellite image compression". Paper presented at the *7th International Workshop on On-Board Payload Data Compression (OBPDC 2020)*.
Available on: `https://hal.archives-ouvertes.fr/hal-03079863/document`

Thank You!

Satellite imaging system

Instrumental noise model:

- Acquired images are affected by an instrumental noise with a pixel-dependent variance defined, in the spatial domain, as [Mas+18]:

$$\sigma^2{}_n(x,y) = A^2 + B \cdot I_{nf}(x,y)$$

(A, B) are known model parameters.

Instrumental noise restitution:

- Idea: compare each quantized transformed wavelet coefficient to the local expected instrumental noise level computed in the transformed domain and restitute noise [Mas+18].

Variance stabilizing transform:

- To use a model-based denoising method that assumes an additive noise, a variance stabilizing transform (VST) [MF12; Ans48] may also be applied to the noisy image:

$$f(I_r(x,y)) = 2\sqrt{\frac{A^2}{B^2} + \frac{I_n(x,y)}{B} + \frac{3}{8}},$$

Performance Analysis

Impact of the GDN/IGDN replacement and of the filter kernel support in the main autoencoder on performance:

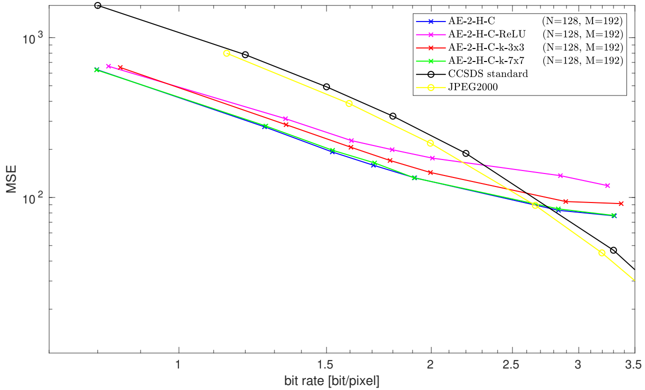

Figure: Impact of the GDN/IGDN replacement and of the filter kernel support on performance in terms of MSE in log-log scale.

Performance Analysis

Impact of the number of layer reduction in the main autoencoder:

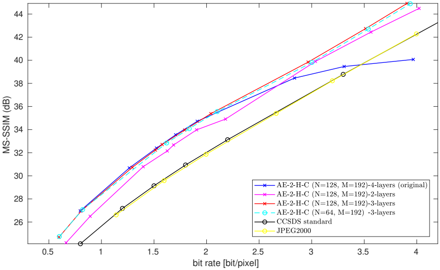

Figure: Impact of the number of layer reduction on performance in terms of MS-SSIM (dB) (derived as $-10\log_{10}(1-\text{MS-SSIM})$).

Table: Comparative complexity of the considered architectures - Case of reducing the number of layers.

Method	Parameters	FLOPp	Relative to FLOPp
AE-2-H-C (N=128, M=192)-4-layers (original)	5055105	1.9115×10^5	1.00
AE-2-H-C (N=64, M=192) -4-layers	1683969	5.2264×10^4	0.27
AE-2-H-C (N=128, M=192)-3-layers	4202625	2.0732×10^5	1.08
AE-2-H-C (N=64, M=192) -3-layers	1470721	6.6605×10^4	0.34
AE-2-H-C (N=128, M=192)-2-layers	3350145	2.7201×10^5	1.42

Performance Analysis

Impact of the simplified Laplacian entropy model in the joint compression and denoising:

- `AE-2-L-CD`: joint learned method featuring the simplified Laplacian entropy model [Alv+21].

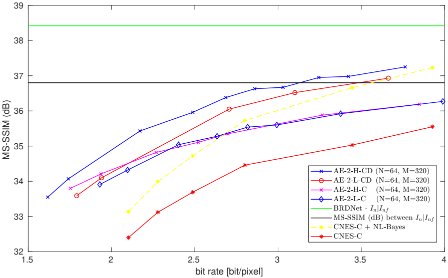

Figure: MS-SSIM (dB) between the output image and the noise-free image ($\mathbf{I_{nf}}$).

Performance analysis

Lower average luminance images:

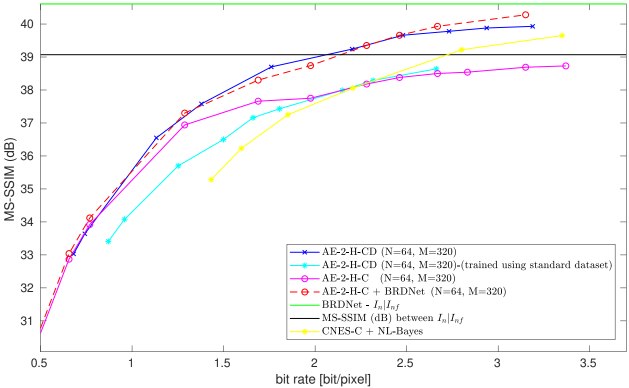

Figure: MS-SSIM (dB) between the output image and the noise-free image ($\mathbf{I_{nf}}$).

References I

[Alv+20] V. Alves de Oliveira, T. Oberlin, M. Chabert, C. Poulliat, B. Mickael, C. Latry, M. Carlavan, S. Henrot, F. Falzon, and R. Camarero. "Simplified entropy model for reduced-complexity end-to-end variational autoencoder with application to on-board satellite image compression". In: *7th International Workshop on On-Board Payload Data Compression (OBPDC 2020)*. 2020, pp. 1–8 (cit. on p. 46).

[Alv+21] V. Alves de Oliveira, M. Chabert, T. Oberlin, C. Poulliat, M. Bruno, C. Latry, M. Carlavan, S. Henrot, F. Falzon, and R. Camarero. "Reduced-Complexity End-to-End Variational Autoencoder for on Board Satellite Image Compression". In: *Remote Sensing* 13.3 (2021). ISSN: 2072-4292. DOI: 10.3390/rs13030447. URL: https://www.mdpi.com/2072-4292/13/3/447 (cit. on pp. 9, 23, 25, 46, 51).

[Alv+22] V. Alves de Oliveira, M. Chabert, T. Oberlin, C. Poulliat, M. Bruno, C. Latry, M. Carlavan, S. Henrot, F. Falzon, and R. Camarero. "Satellite Image Compression and Denoising With Neural Networks". In: *IEEE Geoscience and Remote Sensing Letters* 19 (2022), pp. 1–5. DOI: 10.1109/LGRS.2022.3145992 (cit. on pp. 33, 46).

References II

[Ans48] F. J. Anscombe. "The transformation of Poisson, binomial and negative-binomial data". In: *Biometrika* 35.3/4 (1948), pp. 246–254 (cit. on p. 48).

[Bal+18] J. Ballé, D. Minnen, S. Singh, S. J. Hwang, and N. Johnston. "Variational image compression with a scale hyperprior". In: *International Conference on Learning Representations (ICLR)* (2018) (cit. on pp. 14, 16, 19, 23–25, 36, 44).

[Ben09] Y. Bengio. "Learning deep architectures for AI". In: *Foundations and trends in Machine Learning* 2.1 (2009), pp. 1–127 (cit. on pp. 5–7).

[BLS17] J. Ballé, V. Laparra, and E. Simoncelli. "End-to-end optimized image compression". In: *International Conference on Learning Representations (ICLR)* (2017) (cit. on pp. 10, 13–15, 19, 25, 44).

[Boo17] B. Book. "Consultative Committee for Space Data Systems (CCSDS), Image Data Compression CCSDS 122.0-B-2, ser. Blue Book". In: *CCSDS Secretariat* (2017) (cit. on pp. 3, 25).

[Del+19] J.-M. Delvit, C. Thiebaut, C. Latry, G. Blanchet, and R. Camarero. "A pipeline to improve compressed image quality". In: *International Conference on Space Optics—ICSO 2018*. Vol. 11180. International Society for Optics and Photonics. 2019, p. 111807I (cit. on pp. 2, 18, 34, 35, 39, 42).

References III

[Mas+18] A. Masse, S. Lefevre, R. Binet, S. Artigues, G. Blanchet, and S. Baillarin. "Denoising very high resolution optical remote sensing images: Application and optimization of non local bayes method". In: *IEEE Journal of Selected Topics in Applied Earth Observations and Remote Sensing* 11.3 (2018), pp. 691–700 (cit. on pp. 34, 39, 48).

[MF12] M. Makitalo and A. Foi. "Optimal inversion of the generalized Anscombe transformation for Poisson-Gaussian noise". In: *IEEE transactions on image processing* 22.1 (2012), pp. 91–103 (cit. on p. 48).

[PG81] J. W. Pratt and J. D. Gibbons. "Kolmogorov-Smirnov two-sample tests". In: *Concepts of Nonparametric Theory* (1981), pp. 318–344 (cit. on p. 19).

[Thi+16] C. Thiebaut, C. Latry, R. Camarero, J.-M. Delvit, G. Blanchet, X. Delaunay, E. Bousquet, and G. Lauren. "Performances of a CCSDS-based algorithm for quality- controlled compression on Earth observation missions". In: *5th International Workshop on On-Board Payload Data Compression (OBPDC 2016)*. 2016 (cit. on pp. 3, 39).

[TMB05] D. Tretter, N. Memon, and C. Bouman. "Multispectral image coding". In: *The Image and Video Processing Handbook. sl: Academic Press, London*. 2005 (cit. on p. 4).

References IV

[TXZ20] C. Tian, Y. Xu, and W. Zuo. "Image denoising using deep CNN with batch renormalization". In: *Neural Networks* 121 (2020), pp. 461–473 (cit. on pp. 37, 39, 42).